Bioorganic & Medicinal Chemistry 20 (2012) 5110–5116

Contents lists available at SciVerse ScienceDirect

Bioorganic & Medicinal Chemistry

journal homepage: www.elsevier.com/locate/bmc

Novel structural insights for imidoselenocarbamates with antitumoral activity related to their ability to generate methylselenol

María Font [a,*], Alicia Zuazo [a,b], Elena Ansó [b], Daniel Plano [c], Carmen Sanmartín [c], Juan-Antonio Palop [c], Juan-José Martínez-Irujo [b]

[a] Sección de Modelización Molecular, Departamento de Química Orgánica y Farmacéutica, University of Navarra, Irunlarrea 1, E-31008 Pamplona, Spain
[b] Departamento de Bioquímica y Biología Molecular, University of Navarra, Irunlarrea 1, E-31008 Pamplona, Spain
[c] Sección de Síntesis, Departamento de Química Orgánica y Farmacéutica, University of Navarra, Irunlarrea 1, E-31008 Pamplona, Spain

ARTICLE INFO

Article history:
Received 7 May 2012
Revised 27 June 2012
Accepted 6 July 2012
Available online 15 July 2012

Keywords:
Selenium
Pro-apoptotic
Methylselenol release
Structural variations

ABSTRACT

In the search for molecules with potential antiangiogenic activity we found that several imidoselenocarbamate derivatives, which have pro-apoptotic and antiproliferative activities, under hypoxic conditions release methylselenol, a volatile and highly reactive gas that was considered to be responsible for the observed biological activity. The kinetic for the liberation of methylselenol is highly dependent on the nature of the overall structure and correlate with their proven pro-apoptotic activity in lung cancer cell line H157. The preliminary structure–activity relationships allow us to select as the basic structural element a scaffold constructed with an imidoselenocarbamate fragment decorated with a methyl residue on the Se central atom and two heteroaromatic lateral rings. These imidoselenocarbamate derivatives may be of interest both for their antitumoral activities and because they have a structure that can be considered as a template for the design of new derivatives with apoptotic activity. This activity is related to the controlled delivery of methylselenol and makes this an interesting approach to develop new antitumoral agents.

1. Introduction

Selenium (Se) is an essential micronutrient that is preferably incorporated within a protein type known as the selenoproteins, some of which have antioxidant properties that can prevent cellular damage caused by, for example, some products of oxygen metabolism.[1,2] The expected beneficial effect of selenium, particularly the anticancer properties associated with supranutritional doses of Se,[3] has resulted in the increased popularity of Se as a dietary supplement. However, in recent years these effects have become the subject of great debate due to the fact that the different studies carried out have not allowed definitive conclusions to be drawn.[4–7] These discrepancies can be explained, at least to some extent, by the form of the selenium (i.e. either organic or inorganic) used in the different trials. In fact, in recent years it has been demonstrated that the form of Se is crucial in demonstrating possible beneficial effects since different forms of Se follow different metabolic pathways and it is generally accepted that Se metabolites are responsible for the biological activities of dietary Se supplements.[8,9] As an example, selenite is an inorganic form of selenium that has a cytotoxic effect against several human cancer cell lines and one or more selenite metabolites are considered to be responsible for this toxicity.[10–14]

The most widely studied Se derivatives are organic and these include some selenoaminoacids[15–17] such as selenomethionine (SeMet) or methylselenocysteine (MeSeCys), two Se forms that are processed in some human cancer cells. The data obtained show that MeSeCys killed more lung cancer cells than SeMet and lung cancer cells treated with MeSeCys processed the selenium differently than cells treated with SeMet.[18] MeSeCys is generally more toxic than SeMet, presumably due to its metabolism to methylselenol (MeSeH; at pH 7.4 probably present as methylselenide), an antitumorigenic compound and putative superoxide generator, whereas SeMet is adventitiously incorporated into selenoproteins in place of methionine.[19–22]

It has been hypothesized that MeSeH is a critical selenium metabolite for anticancer activity in vivo, and differential chemopreventive effects of MeSeH on cancerous and noncancerous cells may play an important role.[23–25] Other Se metabolites, such as hydrogen selenide or seleno-diglutathione, can be anti-carcinogenic by inhibiting cell proliferation, stimulating cell death by apoptosis, and inhibiting neoangiogenesis.

Bearing the above information in mind, a novel approach for cancer therapy could be based on the toxic pro-oxidant property of MeSeH, a compound that can be released from some Se-organic derivatives. These compounds could thus act as pro-drugs and this approach is similar to the strategies developed in the early 2000s related to the activity of seleno-L-methionine in cancer therapy.[26] Indeed, previous work on mono-methyl selenium compounds that

* Corresponding author. Tel.: +34 948 425 600; fax: +34 948 425 649.
E-mail address: mfont@unav.es (M. Font).

0968-0896/$ - see front matter © 2012 Elsevier Ltd. All rights reserved.
http://dx.doi.org/10.1016/j.bmc.2012.07.013

are putative precursors of MeSeH has strongly implicated this metabolite in the induction of caspase-mediated apoptosis of human prostate carcinoma and leukemia cells and G1 arrest in human vascular endothelial and cancer epithelial cells.[27] Induction of apoptosis and inhibition of cell proliferation are considered to be important cellular events that can account for the cancer preventive effects of selenium.[28]

In this research area we have developed a number of selenium derivatives with interesting biological profiles as antitumoral agents.[29–32] For example, in the search for molecules with potential antiangiogenic activity we found that several imidoselenocarbamate derivatives (see Table 1) effectively suppress the expression of vascular endothelial growth factor (VEGF) induced by hypoxia in NCI-H157 tumour cells. These compounds did not affect the classical pathways that regulate HIF-1alpha expression, but inhibited STAT3 phosphorylation triggered by hypoxia, thus blocking the synthesis of VEGF. Moreover, these compounds showed interesting antiproliferative and apoptotic activities.[33,34]

In our investigations into the action mechanism of these imidoselenocarbamate derivatives we demonstrated that under hypoxic conditions several of them release MeSeH. The kinetics of this liberation were found to be highly dependent on the nature of the substituent radicals and correlated with their proven pro-apoptotic activity in lung cancer cell line H157 (Fig. 1 and Table 2, previously reported data[33,34]). The kinetics for the release of free alkylselenols were determined by Ellman's Test.[35]

Our data support the initial proposal that MeSeH is responsible for the biological activity of several of these compounds. The imidoselenocarbamate derivatives described here may be of interest both for their antitumoral activities and because they provide a structure that can be considered as a template for the design of new derivatives with apoptotic activity related to the controlled delivery of methylselenol.

We subsequently carried out a molecular modelling study in an effort to gain new insights into the structure–activity relationships for these compounds.

The first objective of the molecular modelling approaches that were applied in the study was to obtain descriptors that would allow us to relate the molecular structural variations to the possibility of the MeSeH release, on the hypothesis that this metabolite is the active agent and the whole imidoselenocarbamate derivative acts as a pro-drug.

On the basis of this hypothesis, we planned to study a number of quantum parameters related to the possible hydrolysis of the C**1**–X bond (See Fig. 2), that is, location, orbital atomic contribution and energy for HOMO and LUMO, net atomic charge at C**1** and X and bond order for the C**1**–X bond. Secondly, a conformational analysis was carried out in order to obtain some insights into the possible influence that the conformational behaviour has on the accessibility of the hydrolysis point, C**1**.

The calculations were performed on a Dell Precision 380 workstation, provided with the software package Discovery Studio v2.5[36] and on an SGI Virtu VS100 workstation, provided with MOPAC2009[37] and Mercury[38] software packages.

In order to facilitate the understanding of the results concerning the effect of the structural modifications on the target activity, the previously reported activity data and a description of the biological methods are included as Supplementary data.

Table 1
Structure of analyzed imidoselenocarbamate and imidothiocarbamate derivatives[a]

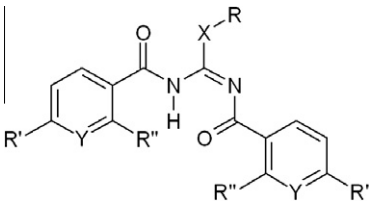

Compd	X	R	R′	R″	Y
1a	Se	CH_3	H	H	C
1b	S	CH_3	H	H	C
1c	Se	C_2H_5	H	H	C
1d	Se	$CH(CH_3)_2$	H	H	C
1e	Se	CH_3	CH_3O	CH_3O	C
1f	Se	$CH(CH_3)_2$	CH_3O	CH_3O	C
1g	Se	CH_3	Cl	H	C
1h	Se	$CH(CH_3)_2$	Cl	H	C
1i	Se	CH_3	NO_2	H	C
1j	Se	CH_3	CF_3	H	C
1k	Se	CH_3	CN	H	C
1l	Se	CH_3	$C(CH_3)_3$	H	C
1m	Se	CH_3	CH_3	H	C
1n[b]	Se	CH_3		$-CH_3-$	
1o	S	CH_3	$C(CH_3)_3$	H	C
1p	S	CH_3	Cl	H	C
1q	S	CH_3	H	H	N
1r	Se	CH_3	H	H	N
1s	S	CH_3	H	Cl	N
1t	Se	CH_3	H	Cl	N

[a] Previously reported.[31]
[b] Aromatic rings replaced by a methyl fragment.

2. Results and discussion

The compounds under investigation correspond to a general structure that incorporates a common scaffold, which is constructed by two planar pi rings located at the ends of an imidoselenocarbamate or imidothiocarbamate fragment. This scaffold is decorated by alkyl chains with different lengths and volumes (from methyl to 2-propyl) located at the central Se/S atom. The lateral aromatic (phenyl) or heteroaromatic (pyridine) rings bear different substituents with electron-donating or electron-withdrawing effects, preferably at position 4, and these modify the electronic contribution and the volume in the host rings. As a reference structure, and in an attempt to establish the smallest effective compound, we prepared a derivative in which the lateral rings are replaced by a methyl group.

Bearing in mind the high degree of conformational freedom estimated for the analyzed structures, we proposed three different starting conformations for the conformational analysis (Fig. 3A–C). The analysis was carried out, having first selected the rotatable bonds (Fig. 3D), by applying the Diverse Conformation Generation protocol implemented in the DS 2.5v suite. A set of 25–30 representative low energy conformations for each analyzed compound was selected (the energy differences between the different conformations analyzed for each trajectory were in the range 2–5 kcal; data not shown for the sake of brevity).

The low energy conformers were superimposed as appropriate onto the central scaffold, with the Se, C**1**, N**2**, N**2**′, C**3** and C**3**′ taken as tethers (Fig. 3D). The effectiveness of the superimposed models was evaluated in terms of the root mean square (rms) values obtained.

The mechano-quantic analysis of the conformations obtained in the previous step was carried out with the package Mopac2009. The atomic orbital contribution, distribution and energy of the HOMO and LUMO orbitals, the net atomic charges for X (Se or S), C**1**, N**2**, N**2**′, C**3** and C**3**′ atoms (Coulson type charges), and the bond order for the C**1**–X bond were obtained for each of the selected conformations, with its optimized geometries using an eigenvector-following

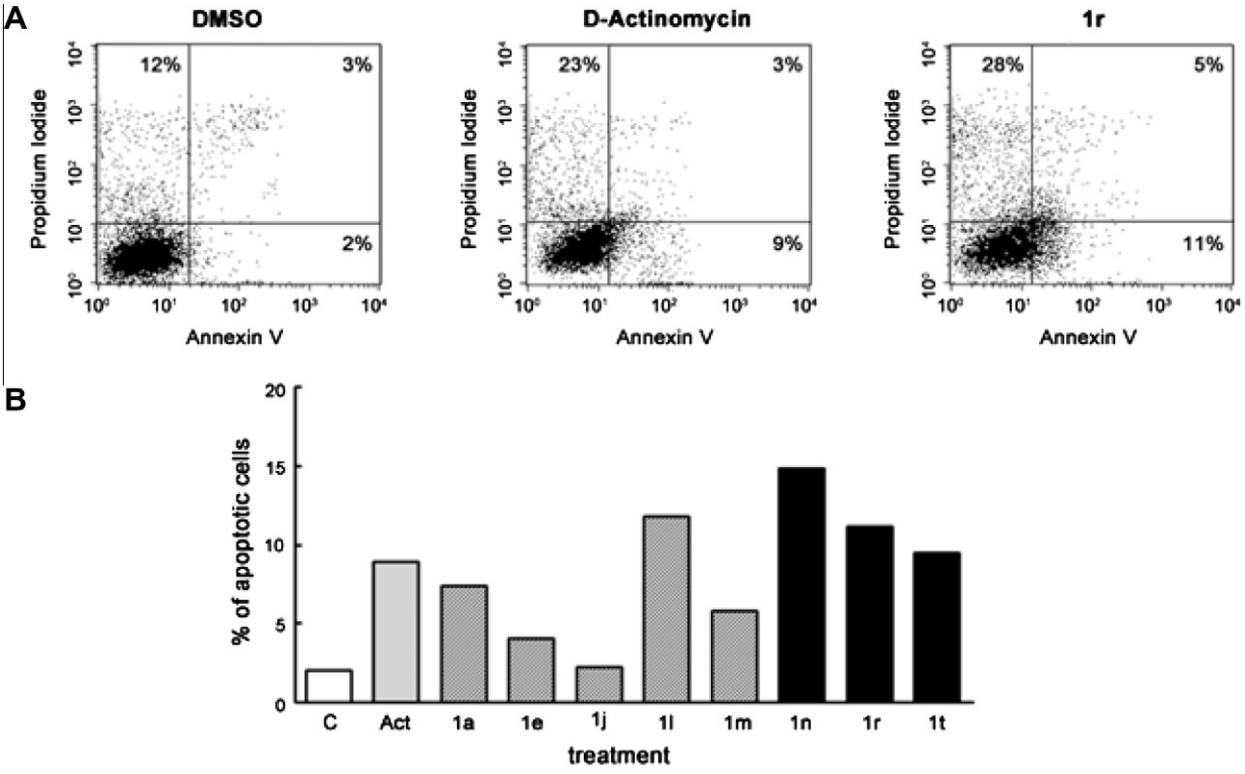

Figure 1. Induction of apoptosis by evaluated derivatives in lung cancer cell line H157. Cells were treated with 10 μM of the indicated compounds for 5 hours in serum-free medium. (A) Representative flow cytogram of annexin V binding (abscissa) versus propidium iodide uptake (ordinate). The numbers in the upper left quadrant, upper right quadrant, lower left quadrant, and lower right quadrant represent the percentage of damaged (annexin V−/PI+), necrotic (annexin V+/PI+), live (annexin V−/PI−) and apoptotic cells (annexin V+/PI−), respectively. (B) Percentage of apoptotic cells (annexin V-positive) after treatment with vehicle (0.5% DMSO), actinomycin D (positive control) and selected imidoselenocarbamate derivatives. (Black bars: compounds with fast MeSeH release; Striped bars: compounds with slow or zero MeSeH release).

Table 2
Methylselenol release kinetics for selected imidoseleno and imidothiocarbamate derivatives[a]

Compd	Phosphate buffer [b]			RPMI medium[c]		
	k (h^{-1})	R^2	$t_{1/2}$ (h)	k (h^{-1})	R^2	$t_{1/2}$ (h)
1n	0.075 ± 0.001	0.998	9.2	0.84 ± 0.07	0.973	0.82
1r	0.026 ± 0.001	0.996	26	0.24 ± 0.01	0.999	2.9
1t	0.017 ± 0.001	0.998	40	0.15 ± 0.01	0.992	4.7
1s	0.00075 ± 0.00004	0.962	917	0.023 ± 0.001	0.996	31
1q	0.00052 ± 0.00003	0.940	1333	0.033 ± 0.001	0.981	24

[a] Table shows the first order rate constants for the release of methylselenol for tested derivatives, as determined by Ellmańs method according to previously reported methods; Reactions were performed in normoxia at room temperature. k represents the first order rate constant of the reaction; $t_{1/2,}$ the half life of the reaction and R^2 the goodness of fit.

[b] 100 mM Na_2PO_4, 1 mM EDTA and 100 μM DTNB (pH 8).

[c] Phenol-red-free RPMI 1640 medium containing 100 μM DTNB (BioWhittaker)

algorithm (PM3 semi-empirical approach).[39] The data (see Table 3) corresponding to the mean value of the representative low energy conformations, selected from the conformational trajectory for each compound, were used to establish the preliminary structure–activity relationships (SAR).

Two different approaches were used to establish this preliminary SAR. Firstly, we considered the structures of compounds with a global form, valuing the influence of the proposed structural modifications progressively along with the conformational behaviour. Secondly, and according to our initial hypothesis that relates the compound activities to their capacity to release methylselenol, we analyzed the possible influence that structural variations carried out for the imidoselenocarbamate derivatives have on the kinetics of the release.

We demonstrated previously[33,34] that the presence of Se is essential for all of the evaluated biological activities, since substitution of Se by S led to complete loss of activity. Thus, comparison of the activity data obtained for the pairs of analogous skeletal derivatives (**1a** vs **1b**, **1r** vs **1q** and **1t** vs **1s**) showed that, while the selenium derivatives show the target activity [IC_{50} = 2.4 μM in the inhibition of hypoxia-induced VEGF expression, a LD_{50} = 4.0 μM and 5.8 μM in the cell viability assay (hypoxic and

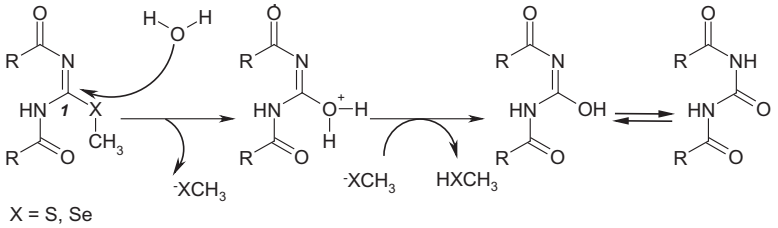

Figure 2. Proposed mechanism for the MeSH and MeSeH release.

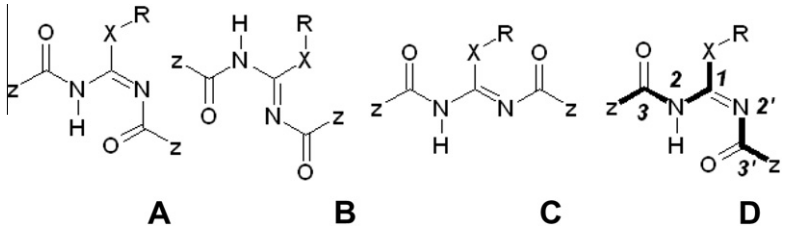

Figure 3. **A**, **B** and **C**, starting conformations for the conformational analysis carried out. **D**: solid line, selected rotatable bonds and central scaffold atoms taken as tethers.

Table 3
Quantum parameters for the analyzed compounds[a]

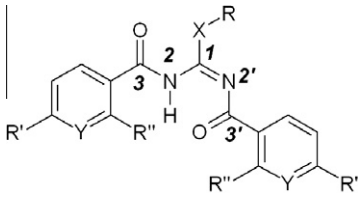

Compd	X	R	R′	R″	Y	C1	X	N2	C3	N2′	C3′	b.o.[b]	E_{HOMO}[c]	E_{LUMO}[c]	$\Delta E_{L\text{-}H}$[c]	Vol[d]	Log *S*[e]	*S*log *P*[f]	Dipole[g]
1a	Se	CH_3	H	H	C	−0.090	0.242	0.084	0.292	−0.203	0.315	0.89005	−9.1559	−1.2097	7.9462	871.26	−4.1123	2.3651	3.0003
1b	S	CH_3	H	H	C	−0.047	0.096	0.008	0.350	−0.196	0.372	0.98138	−9.4783	−0.9065	8.5718	885.98	−5.2161	2.9758	4.7116
1c	Se	CH_2 CH_3	H	H	C	−0.104	0.236	0.087	0.291	−0.205	0.314	0.89085	−9.1006	−1.1682	7.9324	921.39	−4.4395	2.7552	2.8478
1d	Se	$CH(CH_3)_2$	H	H	C	−0.099	0.226	0.069	0.296	−0.204	0.312	0.89171	−8.8771	−1.1807	7.6964	964.03	−4.7668	3.1453	2.6877
1e	Se	CH_3	CH_3O	CH_3O	C	−0.111	0.264	0.111	0.740	−0.219	0.313	0.98345	−9.0184	−1.2675	7.7509	1174.46	−4.3139	2.3995	4.2059
1f	Se	$CH(CH_3)_2$	CH_3O	CH_3O	C	−0.097	0.221	0.072	0.287	−0.200	0.308	0.94939	−9.0092	−−1.3002	7.7090	1267.21	−4.2319	2.9743	2.1271
1g	Se	CH_3	H	Cl	C	−0.088	0.244	0.083	0.292	−0.205	0.314	0.93450	−9.0689	−1.1915	7.8774	966.97	−4.3139	2.3995	2.6939
1h	Se	$CH(CH_3)_2$	H	Cl	C	−0.097	0.232	0.074	0.292	−0.205	0.312	0.91413	−8.8455	−1.1475	7.6980	1016.00	−4.9683	3.1797	2.3806
1i	Se	CH_3	H	NO_2	C	−0.095	0.267	0.093	0.279	−0.206	0.299	0.96612	−9.1900	−1.3190	7.8710	1005.58	−5.5809	3.6719	2.9085
1j	Se	CH_3	H	CF_3	C	−0.090	0.250	0.086	0.283	−0.200	0.306	0.93941	−8.9409	−1.2939	7.6470	1037.49	−6.2353	4.4521	2.7428
1k	Se	CH_3	H	CN	C	−0.106	0.265	0.104	0.283	−0.221	0.312	0.93821	−9.7837	−2.0753	7.7084	996.91	−5.6928	2.1815	4.1104
1l	Se	CH_3	H	$C(CH_3)_2$	C	−0.085	0.236	0.084	0.292	−0.204	0.317	0.98360	−9.5763	−1.6434	7.9329	1245.57	−6.2254	5.0257	3.2122
1m	Se	CH_3	H	CH_3	C	−0.093	0.246	0.083	0.295	−0.206	0.317	0.93185	−9.5988	−1.7352	7.8636	985.14	−4.8142	2.1085	1.2438
1n	Se	CH_3	CH_3			−0.092	0.244	0.084	−0.214	0.266	0.239	0.90952	−9.0741	−1.1534	7.9207	553.07	−8.1515	4.9601	3.1611
1o	S	CH_3	H	$C(CH_3)_2$	C	−0.055	0.106	0.016	0.303	−0.195	0.368	0.98393	−9.0667	−1.1594	7.9073	1251.79	−5.0602	2.9819	3.1262
1p	S	CH_3	H	Cl	C	−0.042	0.100	−0.021	0.311	−0.191	0.371	0.94694	−9.2831	−1.2753	8.0078	967.98	−6.6847	4.2826	2.6848
1q	S	CH_3	H	H	N	−0.094	0.076	−0.031	0.317	−0.096	0.364	0.92871	−9.4152	−0.8389	8.5763	840.28	−9.2553	5.5708	4.9661
1r	Se	CH_3	H	H	N	−0.093	0.255	0.086	0.296	−0.205	0.318	0.89537	−9.3797	−0.9612	8.4185	847.96	−6.6847	4.2826	5.1790
1s	S	CH_3	Cl	H	N	−0.074	0.080	−0.042	0.311	−0.132	0.362	0.98162	−9.5898	−0.8861	8.7037	928.33	−2.6999	1.7658	5.6481
1t	Se	CH_3	Cl	H	N	−0.091	0.253	0.082	0.296	−0.203	0.315	0.83827	−9.3796	−1.4132	7.9664	914.92	−1.5961	1.1551	4,2385

[a] PM3 semiempirical calculation, mean values from the lower energy conformations.
[b] b.o. = X–C1 bond order.
[c] eV.
[d] Å^3.
[e] Log of the aqueous solubility (mol/L).
[f] Log of the octanol/water partition coefficient.
[g] Debyes

normoxic culture conditions, respectively) and GI_{50} = 2.1 μM for **1a**, as a representative example], the analogous thio derivatives are inactive (IC_{50}, LD_{50} and GI_{50} >20 μM for **1b**, as an example).

With regard to the methylselenol release (Table 2), compounds **1n**, **1r** and **1t** quickly release MeSeH, whereas **1a** and **1m** release it slowly and compounds **1e** and **1j** release low levels that are undetected in the screening assay. As can be see in Figure 1, with the exception of **1l**, molecules that quickly release MeSeH show higher amounts of apoptotic cells than those that release MeSeH slowly. The correlation between the rate of MeSeH release and the induction of early apoptosis by imidoselenocarbamates suggests that this compound is responsible for their pro-apoptotic activity. Moreover, the rate of MeSeH generation is markedly influenced by the structural variations carried out.

The accurate quantitative determination of the kinetics of the MeSeH release in compounds **1a** and **1m**, with proven slow-release activity, is difficult since the methylselenol in the presence of oxygen is oxidized to dimethyldiselenide (CH_3-Se-Se-CH_3).

In a preliminary analysis, and according to the descriptors collected in Table 3, the asymmetry in the charge distribution around C**1** is remarkable, with the region formed by atoms N**2** and C**3** having a practically positive value, whereas N**2**′ has a strong negative charge and C**3**′ is positive. On the other hand, a wide range for the global volume values is observed for active compounds.

On considering compounds **1a** (with a moderate pro-apoptotic activity) and **1b** (inactive) as representative examples, one can highlight the marked difference in the positive charge value for Se compared with the charge value for S (0.242 for Se in **1a** derivative and 0.096 for S in **1b**). The Se/S replacement is accompanied by a notable increase in the value of the C**1**–X bond order (b.o.) in the S derivatives (0.98138 for **1b** vs 0.89005 for **1a**). The replacement also brings about a considerable reduction in the water solubility (log *S* = −4.1123 for **1a** and −5.2161 for **1b**) accompanied by a significant increase in the dipole value.

In the imidoselenocarbamate derivatives the distance between the Se and the carbonyl oxygen of C**3** (mean values calculated over

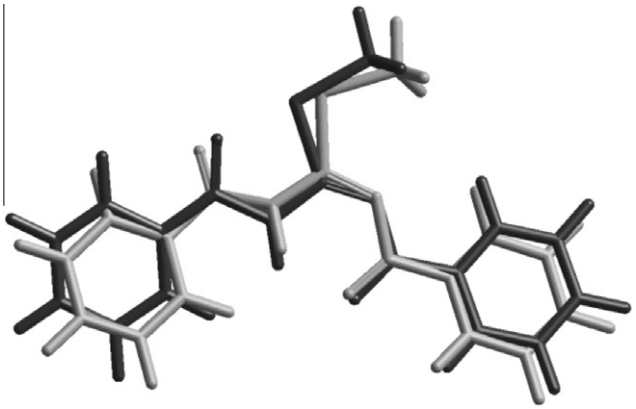

Figure 4. Overlay of representative imidoselenocarbamate **1a** (black) and imidothiocarbamate **1b** (grey), taking atoms C**1**, N**2**, N**2′**, C**3** and C**3′** as tethers.

the lowest energy conformations) is considerably smaller than the value calculated for the thio derivatives (see Fig. 4).

With respect to the alkyl chains located on the central Se atom, the methyl chain is present in all of the active compounds and its replacement by longer chains (ethyl) and/or more voluminous ones (2-propyl) leads to a diminution in the pro-apoptotic activity—with the exception for compound **1l**. As can be observed, the ethyl and 2-propyl chains lead to an increase in the negative charge over the C**1** atom along with a corresponding increase in the C**1**–X b.o. The presence of this longer and/or voluminous chain causes an increase in the Se–O bond distance in a similar way to that observed for S derivatives (data not shown for the sake of brevity) and this also lowers the solubility (see **1a**, **1c** and **1d**, or **1g** and **1h**, Table 3, for representative examples). In addition, the significant decrease in the activity can be related to the progressive increase in the volume of the central section of the scaffold.

The structural simplification carried out on the initial scaffold, that is, the replacement of the lateral rings by a methyl substituent (**1a** vs **1n**), retains the target activity but the theoretical solubility is modified significantly. The C**1**–X b.o. for compound **1n** is similar to that calculated for compound **1a**, although the pro-apoptotic activity of **1n** is higher and is accompanied by a fast MeSeH release. The smaller volume of the residue around the central scaffold element probably facilitates access to the theoretical hydrolysis point.

Regarding the lateral rings that compose the scaffold, a clear relationship could not be established between the electron-withdrawing or electron-donating character of the substituents and the evaluated pro-apoptotic activity. However, it was possible to establish that the presence of any substituent on the lateral phenyl rings makes the liberation of MeSeH difficult. This fact could be related to the higher C**1**–X b.o. values calculated for the substituted phenyl imidoselenocarbamates (Table 3).

The replacement of the phenyl rings by pyridine seems to have a favourable effect on the activity (**1r** vs **1a**) with an insignificant increase in the b.o. value, whereas a significant increase in the

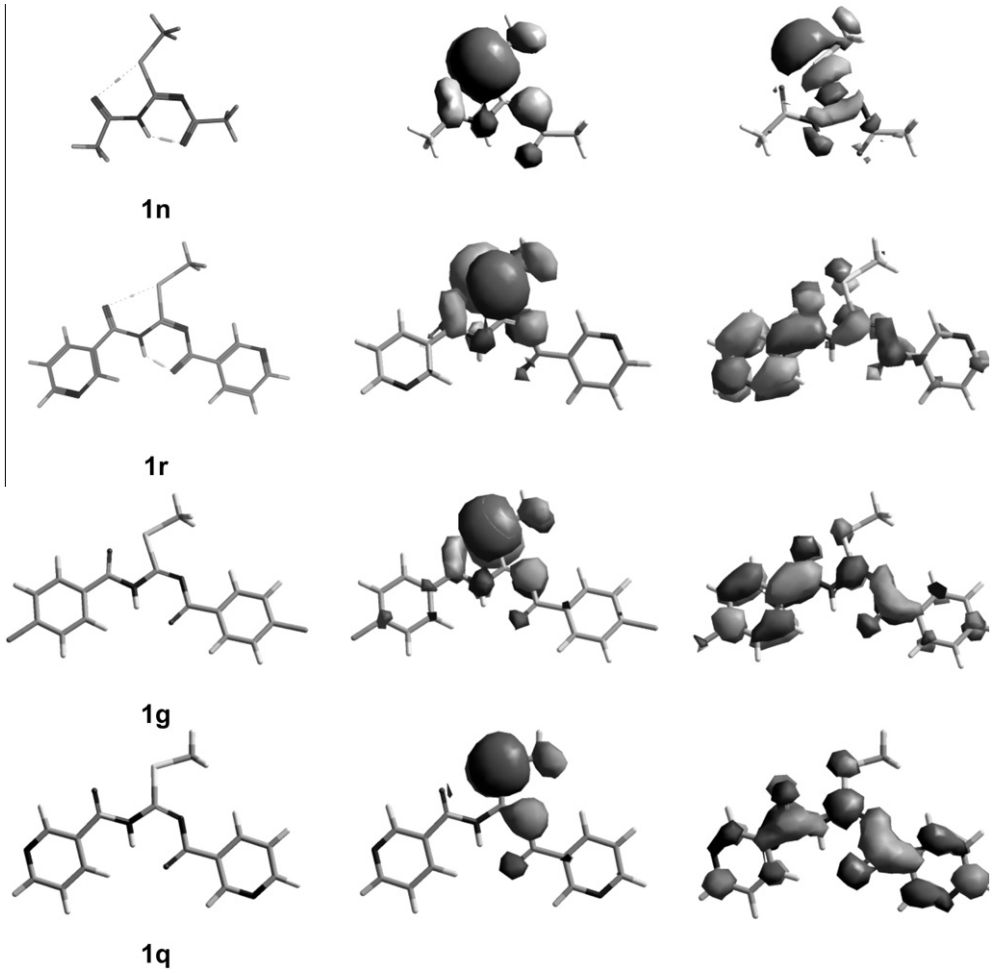

Figure 5. Left: representative lowest energy conformations for active imidoselenocarbamate derivatives **1n** and **1r** (dotted line, noncovalent interaction; solid line: hydrogen bond) and inactive imidoselenocarbamate **1g** and imidothiocarbamate **1q**. Centre: HOMO 0 distribution. Right: LUMO 0 distribution.

dipolar moment can be observed (see **1a** vs **1r**, Table 3). When a Cl atom is introduced into the pyridine ring in the 2 position, the pro-apoptotic activity is maintained (**1r** vs **1t**). As can be observed, the C**1**–X b.o. for pyridine derivative **1t** is the lowest obtained for the analyzed compounds. Both pyridine derivatives show fast MeSeH release and this is accompanied by a significant increase in the theoretical solubility ($\log S = -6.6847$ for **1r** vs -1.5961 for **1t**). Also in this case, the slower release of the active agent, observed for **1t**, could be related to the greater difficulty in accessing the hydrolysis point due to the presence of more voluminous structural elements (Fig. 1, Table 2).

With regard to the conformational behaviour it should be emphasized that an interaction is detected between Se and O3 (Fig. 5). In this noncovalent interaction[40,41] oxygen acts as a nucleophile that approaches Se in a directional manner. Se is an atom with moderate electronegativity and this normally is not expected to interact with electron-donors. The aforementioned interaction is present in 52–63% of the lowest energy conformations analyzed for the imidoselenocarbamates **1a**, **1n**, **1r** and **1t**. In 75% of these selected conformations, this interaction is accompanied by a hydrogen bond formed between the hydrogen of N**2** (HN**2**) and O**3**′ (Fig. 5). The most common conformational family for these derivatives corresponds to the initial conformation type A (Fig. 3). This interaction pattern is modified when the alkyl chain on the Se is ethyl or 2-propyl, in which case only 23–35% of conformations for ethyl derivatives and 18–25% for 2-propyl show the aforementioned interactions. None of the conformations correspond to initial conformation B and only 2–5% of the analyzed conformations correspond to the type C starting conformation.

A similar type of conformational/interactional behaviour is detected for the derivatives with substituents located in the 4-position of the lateral rings. In these cases only a small percentage of the analyzed conformations (close to 15%) display this interaction pattern.

The most pro-apoptotic compounds (related to a faster release of the active agent) demonstrate a clear preference for the conformers in which the double interaction Se–O**3** and HN**2**–O**3**′ is observed, and this could indicate that this interactional schedule may, to some extent, facilitate the hydrolysis and/or the accessibility of the reactive point.

With respect to the analyzed imidothiocarbamates, the most numerous conformational family corresponds to the initial conformation type B (Fig. 3), which has an HN**2**–S hydrogen bond and a noncovalent interaction between N**2** and O**3**. None of the conformations correspond with initial conformation C. Within the conformational type A family, the noncovalent interaction between S and O**3** appears in 20–35% of the conformations accompanied by almost 78% with the HN**2**–O**3**′ hydrogen bond.

As far as the molecular orbitals are concerned, it can be observed in Figure 5 that in the active imidoselenocarbamate derivatives the HOMO orbital is located in the central scaffold region, especially on the Se atom with a significant contribution of N**2**, N**2**′, C**3**, O**3**, O**3**′ and the methyl chain. In the derivatives with substituents located in the 4-position of the lateral rings, the Se contribution to the HOMO orbital is smaller and a small contribution of the ring is observed (see **1g** in Fig. 5 for a representative example). In the thio derivatives the HOMO orbital is located on the S, N**2**′ and O**3**′ atoms (see **1q** in Fig. 5 for a representative example). The location and contribution to the LUMO orbital are more homogeneous for all of the studied compounds (Fig. 5).

In order to obtain complementary data, we also evaluated the possible capacity of the ethyl- and 2-propyl-substituted derivatives to liberate ethylselenol and 2-propylselenol, respectively, by applying the Ellman method. The data obtained (not included) confirm the release of these alkylselenols, with similar behaviour to that obtained for the methyl analogues. The corresponding liberation of alkylthiols was also observed when the same protocol was applied to the analyzed imidothiocarbamates **1s** and **1q**, but in those cases the rate of hydrolysis was very slow.

The remarkable increase in reactivity of the Se derivatives versus the corresponding S derivatives confirms the differences in the chemistry of Se and S.[42] In fact, these results again demonstrate the weaker nature of the C–Se bond as compared with the C–S bond.[43]

3. Conclusions

In the search for new selenium derivatives with antitumoral activity, we have developed a series of imidoselenocarbamates with pro-apoptotic activity related to the ability to release MeSeH. These structures can be considered as a departure point for the subsequent development of new agents that can exert their antitumoral activity through the controlled liberation of MeSeH. The preliminary structure–activity relationships allow us to establish the basic structural requirements for activity, that is, a scaffold constructed with an imidoselenocarbamate fragment carrying a methyl residue on the Se central atom and preferably with two alkyl or heteroaromatic lateral rings, selected such that the C**1**–X bond order values are always below 0.9, and a theoretical aqueous solubility (evaluated by logS) below an approximate value of -3.0.

Despite the interesting activity shown by the compound **1n**, this one becomes slightly unstable, making it difficult to use in the biological trials. Now, we are developing a new alkyl derivatives series, in which the proposed structural modulations are intended to improve the stability of the alkyl imidoselenocarbamate derivatives and to achieve, this way, a good antitumoral profile, favoring the controlled MeSeH release.

With these data, a new cycle of design and synthesis of new heteroaryl and alkyl imidoselenocarbamate derivatives and the preliminary evaluation of its biological profile has been carried out.[30,44] The initial data obtained for the new synthesized series confirms our starting design hypothesis.

4. Molecular modelling methods

The initial computational work was performed on a Dell Precision 380 workstation provided with the software package Discovery Studio 2.5v (DS 2.5v) and with the MOPAC2009 package.

The three-dimensional models of the studied compounds were constructed, in the vacuum phase, using atoms and structural fragments from the Viewer module (DS 2.5v) and using the Dreiding force field.[45] Once the starting models had been constructed, a preliminary conformational analysis was carried out. The applied protocol (Diverse Conformational Generation integrated DS 2.5v protocol) can be summed up as follows: (a) Initial construction of the model and first minimization by application of the Dreiding minimize protocol (steepest descent algorithm with a convergence criterion of $10\,e^{-6}$). (b) Application of the routine for conformation generation (first: conjugate-gradient minimization in torsion space; second: conjugate-gradient minimization in Cartesian space; third: Quasi-Newton minimization in Cartesian space). (c) Elimination of those conformations whose relative energy is greater than 5 kcal/mol at a global minimum. (d) Analysis of conformational trajectory and selection of representative lowest energy conformations. Root mean square (rms) deviations of the structures were monitored. The energy differences between the different conformations analyzed for each trajectory were around 5 kcal.

For each of the compounds, 25–30 lowest energy conformations were selected and a new minimization cycle was applied. The volumes of the whole molecule were also calculated.

The mechano-quantic analysis of the conformations obtained in the previous step was carried out with the package Mopac2009, using the PM3 semi-empirical approach, with the geometry opti-

mized using an eigenvector following algorithm. The atomic orbital contribution, the energy and distribution of the HOMO and LUMO orbitals, the atomic charges (net atomic Coulson type charges), and the bond order was calculated.

As complementary data, the log of the aqueous solubility (mol/L), log*S*,[46] the log of the octanol/water partition coefficient, *S*log*P*[47] and Dipole values were obtained for the analyzed derivatives.

The data corresponding to the mean value of the representative low energy conformations, selected from the conformational trajectory for each compound, were used to establish the preliminary structure–activity relationships.

References and notes

1. Combs, G. F., Jr.; Gray, W. P. *Pharmacol. Ther.* **1998**, *79*, 179.
2. Amaral, A. F. S.; Cantor, K. P.; Silverman, D. T.; Malats, N. *Cancer Epidemiol. Biomark. Prev.* **2010**, *19*, 2407.
3. Alaejos, M. S.; Diaz Romero, F. J.; Diaz Romero, C. *Nutrition* **2000**, *16*, 376.
4. Stratton, M. S.; Algotar, A. M.; Ranger-Moore, J.; Stratton, S. P.; Slate, E. H.; Hsu, C. H.; Thompson, P. A.; Clark, L. C.; Ahmann, F. R. *Cancer Prev. Res. (Phila.)* **2010**, *3*, 1035.
5. Combs, G. F., Jr. *J. Nutr.* **2005**, *135*, 343.
6. Klein, E. A.; Thompson, I. M., Jr.; Tangen, C. M.; Crowley, J. J.; Lucia, M. S.; Goodman, P. J.; Minasian, L. M.; Ford, L. G.; Parnes, H. L.; Gaziano, J. M.; Karp, D. D.; Walther, P. J.; Klotz, L.; Parsons, J. K.; Chin, J. L.; Darke, A. K.; Lippman, S. M.; Goodman, G. E.; Meyskens, F. L., Jr.; Baker, L. H. *JAMA* **2011**, *306*, 1549.
7. Sanmartin, C.; Plano, D.; Font, M.; Palop, J. A. *Current Med. Chem.* **2011**, *18*, 4635.
8. Ganther, H. E. *Carcinogenesis* **1999**, *20*, 1657.
9. Weekley, C. M.; Aitken, J. B.; Musgrave, I. F.; Harris, H. H. *Biochemistry* **2012**, *51*, 736.
10. Kim, E.; Sohn, S.; Kwon, H.; Kim, S.; Kim, M. *Cancer Res.* **2007**, *67*, 6314.
11. Xiang, N.; Zhao, R.; Zhong, W. *Cancer Chemother. Pharmacol.* **2009**, *63*, 351.
12. Weekley, C. M.; Aitken, J. B.; Vogt, S.; Finney, L. A.; Paterson, D. J.; de Jonge, M. D.; Howard, D. L.; Witting, P. K.; Musgrave, I. F.; Harris, H. H. *J. Am. Chem. Soc.* **2011**, *133*, 18272.
13. Olm, E.; Fernandes, A. P.; Hebert, C.; Rundlöf, A.-K.; Larsen, E. H.; Danielsson, O.; Björnstedt, M. *Proc. Natl. Acad. Sci. U.S.A.* **2009**, *106*, 11400.
14. Wallenberg, M.; Olm, E.; Hebert, C.; Bjornstedt, M.; Fernandes, A. P. *Biochem. J.* **2010**, *429*, 85.
15. Schrauzer, G. N. *J. Nutr.* **2000**, *130*, 1653.
16. Wastney, M. E.; Combs, G. F.; Canfield, W. K.; Taylor, P. R.; Patterson, K. Y.; Hill, D.; Moler, J. E.; Patterson, B. H. *J. Nutr.* **2011**, *141*, 708.
17. Naithani, R. *Mini Rev. Med. Chem.* **2008**, *8*, 657.
18. Weekley, C. M.; Aitken, J. B.; Vogt, S.; Finney, L. A.; Paterson, D. J.; de Jonge, M. D.; Howard, D. L.; Musgrave, I. F.; Harris, H. H. *Biochemistry* **2011**, *50*, 1641.
19. Clark, L. C.; Combs, G. F.; Turnbull, B. W.; Slate, E. H.; Chalker, D. K.; Chow, J.; Davis, L. S.; Glover, R. A.; Graham, G. F.; Gross, E. G.; Krongrad, A.; Lesher, J. L.; Park, H. K.; Sanders, B. B.; Smith, C. L.; Taylor, J. R. *JAMA* **1957**, *1996*, 276.
20. Duffield-Lillico, A. J.; Dalkin, B. L.; Reid, M. E.; Turnbull, B. W.; Slate, E. H.; Jacobs, E. T.; Marshall, J. R.; Clark, L. C. *Br. J. Urol. Int.* **2003**, *91*, 608.
21. Lippman, S. M.; Klein, E. A.; Goodman, P. J.; Lucia, M. S.; Thompson, I. M.; Ford, L. G.; Parnes, H. L.; Minasian, L. M.; Gaziano, J. M.; Hartline, J. A.; Parsons, J. K.; Bearden, J. D., 3rd; Crawford, E. D.; Goodman, G. E.; Claudio, J.; Winquist, E.; Cook, E. D.; Karp, D. D.; Walther, P.; Lieber, M. M.; Kristal, A. R.; Darke, A. K.; Arnold, K. B.; Ganz, P. A.; Santella, R. M.; Albanes, D.; Taylor, P. R.; Probstfield, J. L.; Jagpal, T. J.; Crowley, J. J.; Meyskens, F. L., Jr.; Baker, L. H.; Coltman, C. A., Jr. *JAMA* **2009**, *301*, 39.
22. Larsen, E.; Hansen, M.; Paulin, H.; Moesgaard, S.; Reid, M.; Rayman, M. J. *AOAC Int.* **2004**, *87*, 225.
23. Zeng, H.; Briske-Anderson, M.; Wu, M.; Moyer, M. P. *Nutr. Cancer* **2012**, *64*, 128.
24. Zeng, H.; Wu, M.; Botnen, J. H. *J. Nutr.* **2009**, *139*, 1613.
25. Zeng, H.; Botnen, J. H.; Briske-Anderson, M. *Nutr. Cancer* **2010**, *62*, 85.
26. Yamamoto, N.; Gupta, A.; Xu, M.; Miki, K.; Tsujimoto, Y.; Tsuchiya, H.; Tomita, K.; Moossa, A. R.; Hoffman, R. M. *Cancer Gene Ther.* **2003**, *10*, 445.
27. Wang, Z.; Jiang, C.; Lü, J. *Mol. Carcinog.* **2002**, *34*, 113.
28. Sinha, R.; El-Bayoumy, K. *Curr. Cancer Drug Targets* **2004**, *4*, 13.
29. Moreno, E.; Plano, D.; Lamberto, I.; Font, M.; Encío, I.; Palop, J. A.; Sanmartín, C. *Eur. J. Med. Chem.* **2012**, *47*, 283.
30. Ibáñez, E.; Plano, D.; Font, M.; Calvo, A.; Prior, C.; Palop, J. A.; Sanmartín, C. *Eur. Med. Chem.* **2011**, *46*, 265.
31. Plano, D.; Ibanez, E.; Calvo, A.; Prior, C.; Palop, J. A.; Sanmartin, C. *Molecules* **2011**, *16*, 6349.
32. Plano, D.; Sanmartín, C.; Moreno, E.; Prior, C.; Calvo, A.; Palop, J. A. *Bioorg. Med. Chem. Lett.* **2007**, *17*, 6853.
33. Zuazo, A. Ph. D. Thesis. University of Navarra, Pamplona, Spain, March 2011.
34. Zuazo, A.; Plano, D.; Anso, E.; Font, M.; Martínez-Irujo, J. J. Unpublished results.
35. Ellman, G. L. *Archiv. Biochem. Biophys.* **1958**, *74*, 443.
36. Accerlys Software Inc. Discovery Studio Modeling Environment Release 2.5. Accerlys Software Inc.: San Diego, USA, 2010.
37. MOPAC MOPAC2009, Stewart, J.P. Stewart Computational Chemistry, Colorado Springs, CO, USA, http://OpenMOPAC.net, 2008.
38. Macrae, C. F.; Edgington, P. R.; McCabe, P.; Pidcock, E.; Shields, G. P.; Taylor, R.; Towler, M.; Van de Streek, J. J. *Appl. Crystallogr.* **2006**, *39*, 453.
39. Stewart, J. P. *J. Comput. Chem.* **1989**, *10*, 209.
40. Murray, J. S.; Lane, P.; Politzer, P. *Int. J. Quantum Chem.* **2007**, *107*, 2286.
41. Murray, J. S.; Lane, P.; Politzer, P. *Int. J. Quantum Chem.* **2008**, *108*, 2770.
42. Wessjohann, L. A.; Schneider, A.; Abbas, M.; Brandt, W. *Biol. Chem.* **2007**, *388*, 997.
43. Plano, D.; Lizarraga, E.; Font, M.; Palop, J. A.; Sanmartin, C. J. *Therm. Anal. Colorim.* **2009**, *98*, 559.
44. Ibañez, E.; Agliano, A.; Prior, C.; Nguewa, P.; Redrado, M.; González-Zubeldia, I.; Plano, D.; Palop, J. A.; Sanmartin, C. *Current Med. Chem.* **2012**, *19*, 3031.
45. Mayo, S. L.; Olafson, B. D.; Goddard, W. A. *J. Phys. Chem.* **1990**, *94*, 8897.
46. Hou, T. J.; Xia, K.; Zhang, W.; Xu, X. J. *J. Chem. Inf. Comput. Sci.* **2004**, *44*, 266.
47. Wildman, S. A.; Crippen, G. M. *J. Chem. Inf. Comput. Sci.* **1999**, *39*, 868.